Proceedings of the IMAC-XXVIII
February 1–4, 2010, Jacksonville, Florida USA
©2010 Society for Experimental Mechanics Inc.

Modeling, Estimation, and Monitoring of Force Transmission in Wind Turbines

Colin Haynes, Dept. of Structural Eng, University of California – San Diego
Nick Konchuba, Dept. of Mechanical Eng, Virginia Tech
Gyuhae Park, The Engineering Institute, Los Alamos National Laboratory
Kevin M. Farinholt, The Engineering Institute, Los Alamos National Laboratory

ABSTRACT

Recent studies by the Department of Energy suggest that wind energy could make up as much as 20% of total U.S. power generation by 2030 [1]. By better understanding the load transmission in wind turbines, subsequent improvements in design could result in more efficient turbines and reduced maintenance costs. The objective of this study is twofold. First, a low-cost monitoring system to assess the condition of the bolted joint connections used to attach the blades to the hub is devised in order to characterize the force transmission into the hub and to detect when bolt loosening for in-service wind turbines. A section of the CX100 blade is used for the joint monitoring study. Second, a method to estimate the tip deflection of the blade is developed to better understand the dynamic loads acting on the rotor hub. A one-meter-long blade is used to estimate the tip deflection under laboratory conditions. Using the results from these tests, this study demonstrates how a better understanding of load transmission from the blade to the hub may be achieved.

Introduction

In the coming decades, the number of online wind turbines is expected to increase dramatically as the nation seeks to expand its renewable energy generation. The trend in wind energy is also toward larger, longer, and heavier blades in order to generate more power per unit. With demand increasing and designs growing larger, ensuring the reliability of wind turbine design is of critical importance to achieving the goal of 20% wind power. Although failure in the gearboxes or rotor blades is not the most common type of damage that occurs in wind turbines, it is among the most difficult, time-consuming, and expensive damage to repair [2]. Designers therefore need a better understanding of the forces acting on these devices to develop improved systems. Furthermore, a rotational imbalance due to blade damage can cause serious secondary damage to the turbine if not corrected promptly, emphasizing the need for monitoring to protect against bolt loosening and other damage [3].

In order to monitor the state of a structure and to predict failure before it occurs, modern structures may implement health monitoring. The Structural Health Monitoring (SHM) process would bring significant advantages to the wind turbine application by moving the maintenance paradigm to condition-based maintenance rather than time-based maintenance. The current time-based maintenance might prescribe a set time for replacement of blades or other components, whether or not these components are in need of replacement. However, wind turbines are typically located in remote and windy sites which make them expensive and dangerous to repair. Current inspection techniques cost about two percent of the initial wind turbine cost annually [5]. A SHM system would identify the state of damage of turbine components and reduce the uncertainty associated with time-based maintenance, allowing repairs to be made when a part is actually damaged. Such a system would also mitigate the high cost of unexpected catastrophic failure caused by undetected damage.

Many health monitoring systems rely on the use of “smart” materials called piezoelectrics (PZT) patches. These materials strain when a voltage is applied; conversely an applied strain causes the piezoelectric (in this case, a PZT patch) to produce a charge. In this way, PZT tranducers bonded to a host structure can serve the dual purposes of actuation and sensing and consequentially are called “smart” or “active” materials. PZT wafers are used widely in structural dynamics applications to measure high-frequency dynamic responses because they are

lightweight, inexpensive, and robust. Park et al. reviewed PZT sensors and their application to the impedance method in great detail [6].

To better understand the causes of rotating imbalance and premature gearbox damage, designers are particularly interested in the blade tip deflection and the forces transmitted through the hub to the gearbox. Therefore, methods are proposed here to measure both quantities.

Mascarenas et al. were able to identify loose bolt damage by implementing the impedance method using frequency shifts as a feature for damage identification [4]. A PZT patch bonded to an aluminum washer ('smart washer') was used as a damage detection sensor. A smart washer is advantageous in turbine applications because it is cheap to manufacture compared to other alternatives such as load cells. The simplicity and repeatability of the washer result in the need for only one baseline measurement of the impedance and not a baseline measurement for each washer. The unique aspect of this study is modifying the approach of Mascarenas et al. by implementing the impedance method with a smart washer using damping as a feature for both damage identification and quantifying the static forces transmitted through the hub. A mathematical relationship correlating the damping with the bolt torque is determined so that a simple red-yellow-green light SHM system could be implemented to provide turbine operators a condition-based warning system for loose bolt damage.

In order to monitor the tip deflection of the blades, an accelerometer is applied to the tip of the blade. The acceleration data and a state-space model of the blade structure are the input to a Kalman filter, which will be used to extract the desired deflection [7]. The Kalman filter has several advantages over other possible numerical methods. First, the algorithm does not require knowledge of the initial conditions as do integration routines, which prevents it from diverging over time. Also, the Kalman filter requires no knowledge of the forcing function applied to the structure—quite convenient considering that it is impractical to measure the wind pressure on an actual wind turbine blade. Finally, there is significant robustness with respect to the parameters that make up the model, meaning that not all parameters need to be known exactly to obtain a solution. In this study, the algorithm is subjected to two verification tests: an analytical 2-DOF spring-mass-damper system and an aluminum cantilever beam test. Subjecting the algorithm to a test on an actual wind turbine is the next step in verification.

Experimental Procedures for Loose Bolt Damage Identification

The smart washer shown in Figure 1 first implemented by Mascarenas et al. was used as a bolt damage detection sensor. Initially, an experiment was performed to validate the capabilities of the washer for loose bolt damage identification. Using a CX-100 turbine hub shown in Figure 2, 6 bolts spaced evenly around the hub were tightened to 25 ft-lbs to simulate an undamaged (tight) condition. Five baseline measurements were taken by recording the mechanical impedance of the smart washers under these loads at the washers' first resonant frequency. Bolt/washer assembly labeled 4 was loosened to 0 ft-lbs of torque to simulate a damaged (loose) condition. Then bolts 4 and 9 were loosened to 0 ft-lbs of torque to simulate two bolts in the damaged condition. The impedance of the damaged bolts showed significantly larger resonant amplitudes than the undamaged bolts, indicating that by measuring the impedance of a smart washer, a damage index could be developed to identify which bolts were in the damaged state and undamaged state.

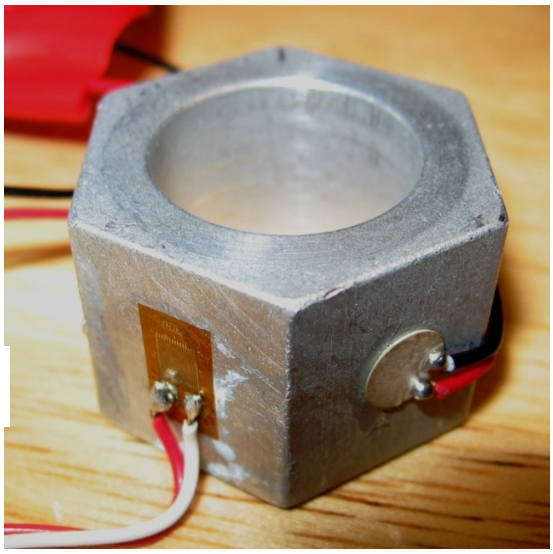

Figure 1 - A smart washer used for damage identification. A PZT patch is bonded on the right, and a strain gauge is bonded on the left.

Secondly, the impedance response of the smart washer was measured under varying bolt torque conditions at the first and second modes. Using the ABAQUS finite element code the mode shapes and frequencies of the first and second mode were estimated. The frequencies estimated were on the order of 20 kHz and 50 kHz.

For the experiment, an Agilent 4294 impedance analyzer was used. The analyzer was connected to the PZT patch on the smart washer. A MATLAB program controlled the operation of the impedance analyzer which actuated the PZT over a frequency range and then sensed the response using the same patch.

Figure 2 - A CX-100 turbine hub, approximately 15" OD, used for testing.

Procedure:

1. Input a frequency range for the first and second modes into MATLAB® program controlling the Agilent® impedance analyzer
2. Measure impedance response with analyzer at first and second modes at each torque level
   (Torque Levels: 0, hand-tight (~1), 5, 10, 15, 20 [ft-lbs])
3. Repeat 1-2 for seven Smart Washers and bolt assemblies

With increasing torque level, a slight shift in natural frequency to higher frequencies and substantial amplitude attenuation were observed in the measurements. Additionally, the 20 kHz mode was lost in noise above 10 ft-lbs and the second mode shows coupled resonance peaks above 10 ft-lbs. The experimental setup was modified to include a piece of rubber isolating the washer and the bolt and the washer and the test plate to isolate structural coupling with the washer dynamics. The experiment was then repeated with the new setup. The first mode was again lost in noise after 10 ft-lbs. The second mode has one resonance peak with greater amplitude attenuation as torque increases. The damping of the second mode was chosen as a good indicator of torque level over the torque test range of interest because the amplitude attenuation is significant between torque levels; however, the rubber isolators resulted in somewhat inconsistent torque measurements. Therefore, a strain gauge was applied to the smart washer and the impedance response of the washer under varying loading conditions was measured after the strain had reached a steady state. The strain was recorded for each impedance measurement. The strain was calibrated with the actual torque in the bolt by recording the strain while the torque in the bolt was maintained with a torque wrench.

Experimental Procedures for Kalman Filter

Tip deflection estimation was accomplished by the application of an algorithm known as the Kalman filter. The Kalman filter allows particular states (e.g. displacement, temperature, strain) to be estimated when it is impossible to obtain direct measurements. A dynamic model of the system must first be produced, which is used by the algorithm together with the measured data to produce the estimates of the desired states. The algorithm itself uses an iterative method that seeks to minimize the variance of the estimation error to predict and update the values of the state variables in each time step of the simulation [7]. There are several significant advantages of using a Kalman filter in the wind turbine application. First, the filter does not require knowledge of the forcing function, which is highly variable and dependent on wind conditions in a turbine. Second, the filter can estimate tip deflection—a quantity that is infeasible to measure directly in a large-scale wind turbine—using only tip acceleration measurements. Furthermore, convergence of the solution does not depend on knowledge of the initial conditions and is robust with respect to variation in parameters (geometrical, material, etc.) whose values are not well known.

The process of tip deflection estimation began with the implementation of the Kalman filter in the Python language. The code was then verified by running simple test problems. The first test problem was an analytical, two DOF spring-mass-damper system with a sinusoidal input applied. The input was assumed to be known, the

"measured" quantity is the displacement of the first mass. The solution from this problem was compared to a known reference solution and the performance of the algorithm was confirmed. Next, the algorithm was modified to use a model constructed from beam finite elements. After assembling the stiffness and mass matrices, the model is converted into a state-space representation and passed to the Kalman filter. Code verification for this revised Kalman filter was accomplished using a rectangular aluminum beam test structure, shown in Figure 3. The beam was fixed on one end and the cantilevered end was 15 cm long. A shaker was attached 5 cm from the fixed end, and an accelerometer and laser vibrometer were placed at the free end of the beam. Three inputs were applied to the beam: a chirp, an impulse chain, and a sine wave. The tip acceleration, tip displacement, and input force data were recorded imported to Python for the data analysis.

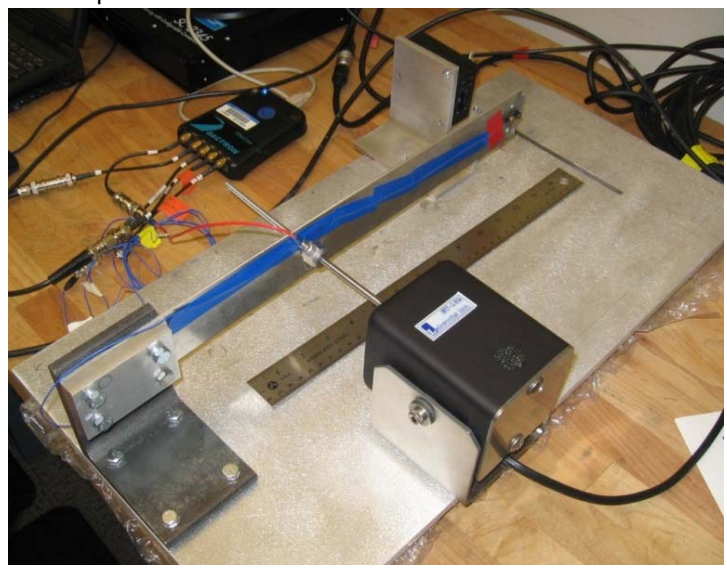

Figure 3 - Aluminum cantilever beam test set-up.

Smart Washer Analytical Modeling

In order to determine the modes and frequencies of the smart washer that is measured by the impedance analysis, an analytical model was constructed. ABAQUS finite element software was used to create the geometry and mesh it with about 5 elements through the thickness at the thinnest point. The meshed model is shown in Figure 4. Then a linear modal analysis was run to determine the frequencies and mode shapes for various boundary conditions.

For initial frequency estimates used to determine a reasonable range for the experiment, the washer was simulated in the free-free condition. Later, attempts were made to replicate the experimental phenomenon of damping and frequency shifts with changing torque in the model. To make a comparison of damping, a frequency response function was obtained by selecting two nodes in the model as well as a frequency range over which the dynamics would be obtained. The output data were then processed to extract the FRF.

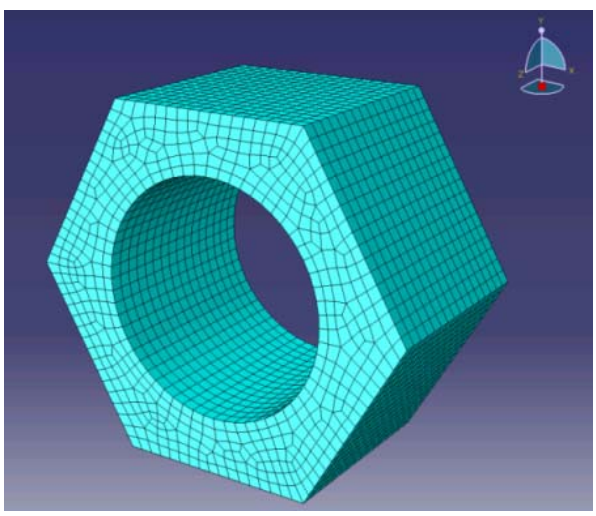

Figure 4 - Finite element model of the washer.

However, it was observed in all cases that the frequency and damping did not change significantly and that whatever change was exhibited was highly dependent on the boundary conditions applied. The washer was first modeled with an applied compressive pressure to simulate the bolt torque, but this boundary condition did not change the frequency response. The washer was then modeled using 3D spring-to-ground elements at each node of the contact faces. The spring stiffnesses were varied, resulting in noticeable changes in frequency. It is hoped that by understanding the boundary conditions better, the model can be calibrated to show better agreement with experimental observations.

Data Analysis - Bolt Joint Monitoring

In the bolt monitoring experiments, the impedance of a smart washer was measured under two loading conditions—loose and tight—to investigate the capacity of a smart washer for identifying loose bolt damage. The smart washer impedance was measured under multiple loading conditions at the first and second modes. In the analysis, the damping of the impedance response is used as the feature to correlate with torque load. The

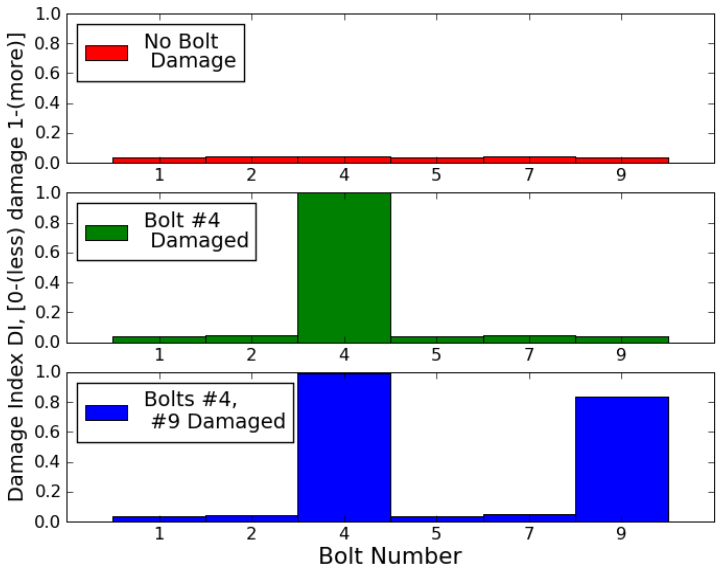

Figure 5 - Damage detection in turbine hub bolted joints.

frequencies from the modal analysis of the washer were used to determine the experimental frequency range. However, as stated in the previous section, the resonance peaks of the first and second mode of the washer become coupled with the test structure and the bolt at higher torque levels; as a result, damping estimation becomes difficult. The washer was isolated from the test structure and the bolt with two pieces of rubber material. Damping was extracted from the impedance response, but results were not repeatable. Finally, a strain gauge was attached to the washer and damping was correlated to the axial strain in the washer.

A simple damage index was developed to demonstrate the effectiveness of a smart washer at detecting damage. The magnitude of the impedance for all data was normalized by the peak amplitude of the loose bolt impedance response; in this way, a damage index of 1 indicated complete loose bolt damage and a 0 indicates infinite bolt torque load. Figure 5 shows the undamaged baseline data (all bolts torqued to 25 ft-lbs) near a damage index of 0. When bolts 4 and 9 are loosened to 0 ft-lbs, the damage index clearly indicates loose bolt damage. There is some variability in the damage index value of bolts 4 and 9; however, the values are relatively close validating the claim that smart washers provide repeatable data.

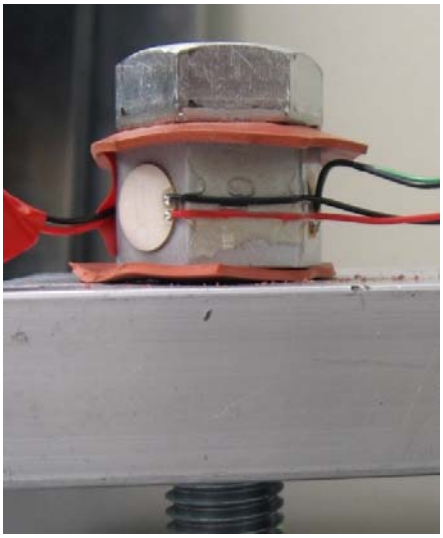

Figure 6 - Test assembly showing the rubber isolators (dark orange) between the bolt and washer and the washer and aluminum test plate.

The next test, which measured the impedance of the washer at varying torques, demonstrated coupling in the impedance response between the structure, bolt, and washer. The half power method was used to calculate the damping of the impedance response at each torque level. A script written in the Python language implemented the half-power method for the experimental data. Another Python script was used to estimate the variability from using the half-power damping method. In this script, the damping ratio of a 1-DOF mass-spring-damper system was varied and the half-power damping script was implemented to estimate the response. The half-power method estimate of damping was determined not to diverge significantly from the true damping value until approximately 10% damping. The damping in the test range of torques was between 0 and 2.5 %; therefore, the half-power method is valid for our test. In addition, the half-power method resulted in only a small amount of error in the torque estimates. The most significant error in torque estimation came from the torque wrench and the rubber isolators. Using a 350 ohm strain gauge in a quarter bridge setup, the torque was correlated with the strain in the bolt. A maximum variability of 2 ft-lbs was determined from our strain-torque calibration. Finding a more suitable damping material than the rubber that would both isolate the washer but demonstrate fewer viscoelastic characteristics might be necessary to implement this measurement method on an actual turbine hub. Curve fitting techniques might also be tried on the impedance response; this might reduce the need for a correlation to strain and the use of the isolators all together.

Figure 7 presents a correlation between damping ratio and bolt torque load. The data in red represents damping measurements when the bolt was damaged (0-1 ft-lbs). The data in blue represents damping measurements

when the bolt undamaged (>1 ft-lbs). All of the damaged data points fell below a damping ratio threshold of 1.25%. In implementing this system on an actual turbine a damping measurement of 1.25% or less would indicate loose bolt damage is present. The undamaged data points were linearly curve fit; all of the data falls between ±2.5 standard deviations from the mean trend line. For any given damping estimate, a range of possible torque values can be identified with close to 95% certainty. As an example, a damping measurement of 2 % would indicate that the torque in the bolt was between 14 and 18 ft-lbs, ± 2 ft-lbs variability.

Previous bolt damage indication systems have used a red light (damaged) - green light (undamaged) system [4]. In order to better service a wind turbine before it becomes damaged, it is advisable to implement an additional 'yellow' light that a bolt is soon to be damaged. In order to design this system several parameters would need to be identified. A minimum torque value would be prescribed based on giving a technician enough time to respond to the warning and fix the loose bolt damage before damage becomes critical. By using the damping ratio to torque relationship established previously, a damping ratio can be selected guaranteeing that if this damping ratio is measured the torque will not be less than the minimum warning torque. Any damping values below this threshold would have to indicate the bolt is damaged. The second parameter that must be established is the minimum torque level which can be considered undamaged. Once this level is established the damping ratios for which the red, yellow, and green light warning indicators represent is completely defined. For illustrative purposes, the red, yellow, green light system is demonstrated on Figure 7 where 6 ft-lbs is the minimum safe torque for potential damage to be fixed, and 14 ft-lbs is the minimum torque for which the turbine blade is safely tightened to the hubs.

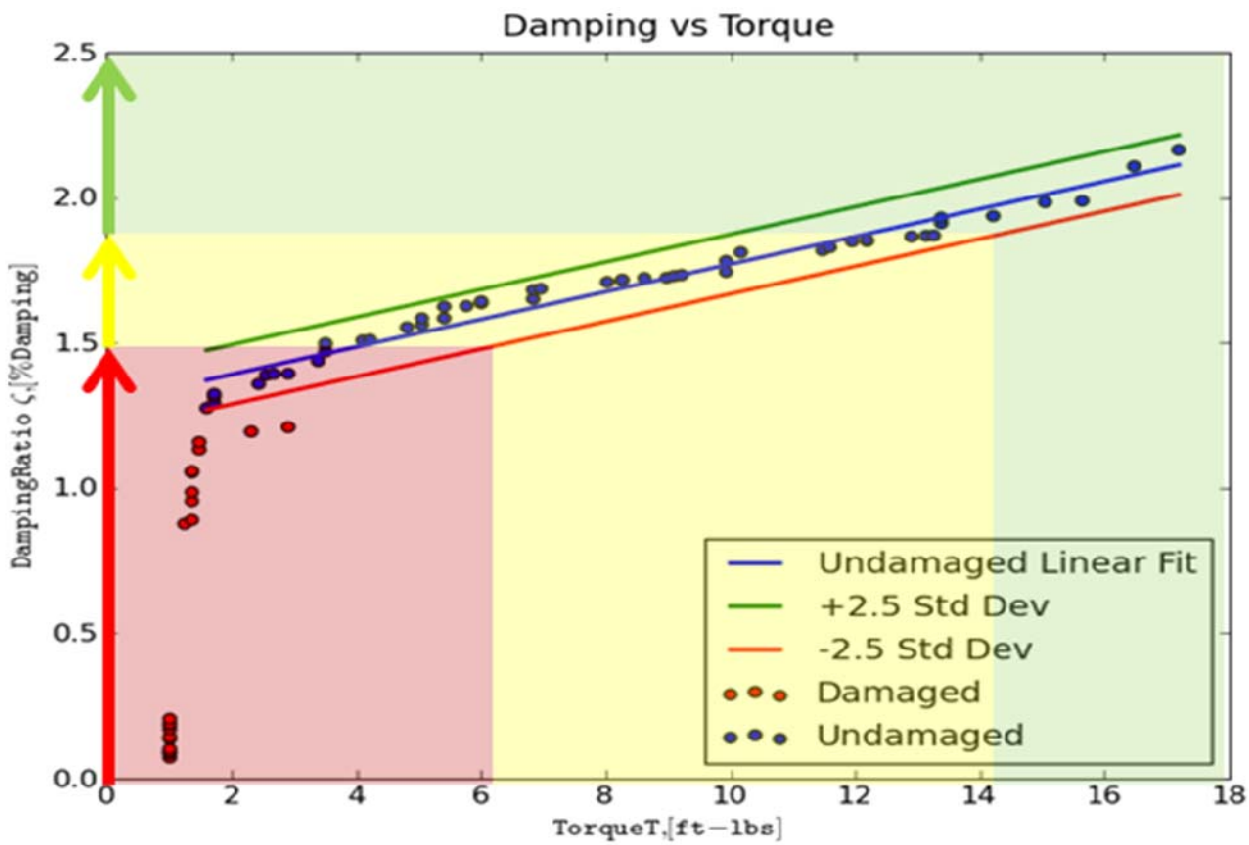

Figure 7 - Correlation between damping ratio and torque. The red, yellow, and green sections show how a potential warning system could be developed for loose bolt damage.

Future work would include improving the variance of the torque measurements by implementing an improved smart washer vibration isolator or curve fitting to eliminate the need for the isolators all together. In addition the following should be investigated: the repeatability and variability of damping-torque curve experiments on the CX-

100 hub, validation of the red-yellow-green light warning system when bolts/washers are on a turbine hub, and the capacity of a smart washer for determining dynamic loads through the hub.

Data Analysis - Kalman Filter

After making measurements on a credible test structure (in this case, the aluminum beam), the data were analyzed. For the Kalman filter, the input force is assumed to be unknown; therefore, the input does not play a role in the algorithm. The measured quantity used for comparison by the filter is the acceleration at the tip of the beam. Finally, the displacement data is not used directly, instead being used as a comparison for the estimated deflection.

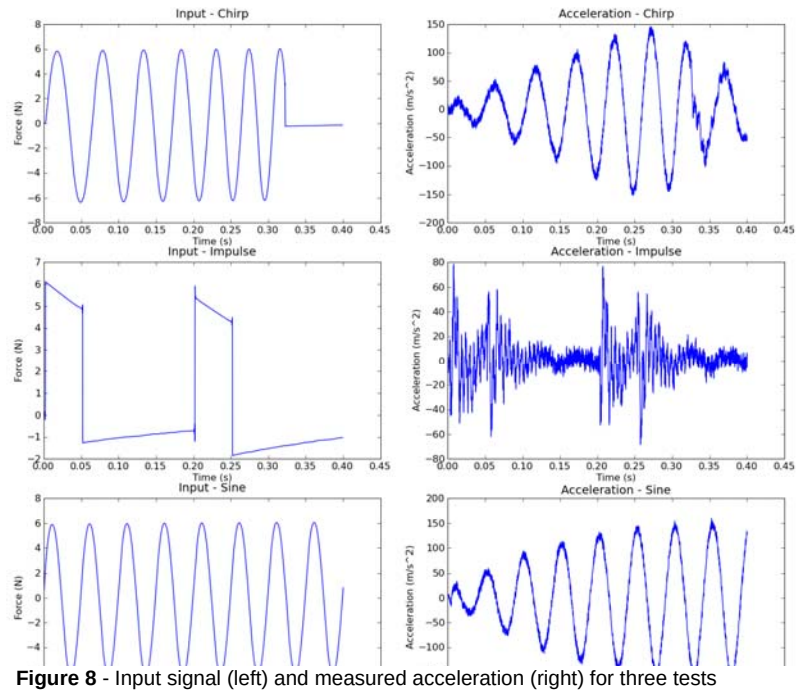

Figure 8 - Input signal (left) and measured acceleration (right) for three tests conducted on the aluminum cantilever beam.

The most notable feature of the input data is the noisiness of the accelerometer data, as shown in Figure 8. This figure shows measurements of force for all three input types in the left column compared to the measured tip acceleration in the right column. Speculation suggested that such high levels of noise might lead to a poor convergence of the Kalman filter solution, but in fact the solution still converged quite well for the chirp and sine inputs. However, the impulse chain input did not converge well, probably because the sudden changes in the (unknown) input combined with noisy accelerometer data did not allow the Kalman filter to adjust properly in the time window being studied. For the remainder of the discussion of the aluminum beam test, the chirp input will be the example chosen.

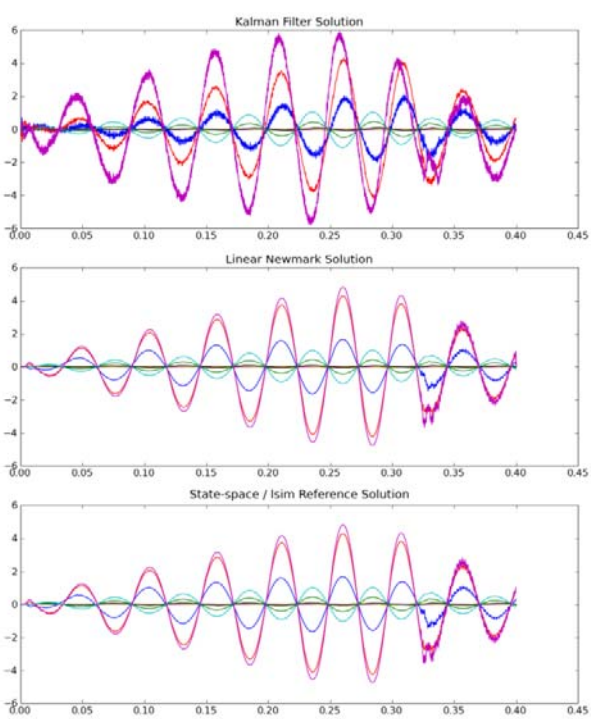

Figure 9 - Comparison of state vector predicted by Kalman filter and by two integration routines.

To further verify the performance of the Kalman filter, the estimated state vector was compared with two separate integrated reference solutions, as shown in Figure 9. It is important to note that integrated solutions will be more accurate in this test application, but are infeasible for use in wind turbines for two reasons. First, unlike the Kalman filter, the integrated solutions require a measurement of the input force. Second, the integrated solutions will begin to diverge over time due to the uncertainty in the initial conditions. The solutions would be sure to diverge in a wind turbine because the initial conditions are not known as they are in the simple beam test and because of the much longer time duration. However, these solutions are useful for comparative purposes, and it can be seen that they agree well.

A more quantitative assessment is obtained by comparing the tip deflection prediction of the Kalman filter to the values measured by the laser vibrometer during the test. This comparison is shown in Figure 10. The error between the measured and predicted values is shown in yellow. The peak value of the deflection is predicted with only a

2.0% error, an encouraging number considering the peak deflection is the quantity of most interest in determining the loads transferred to the wind turbine hub.

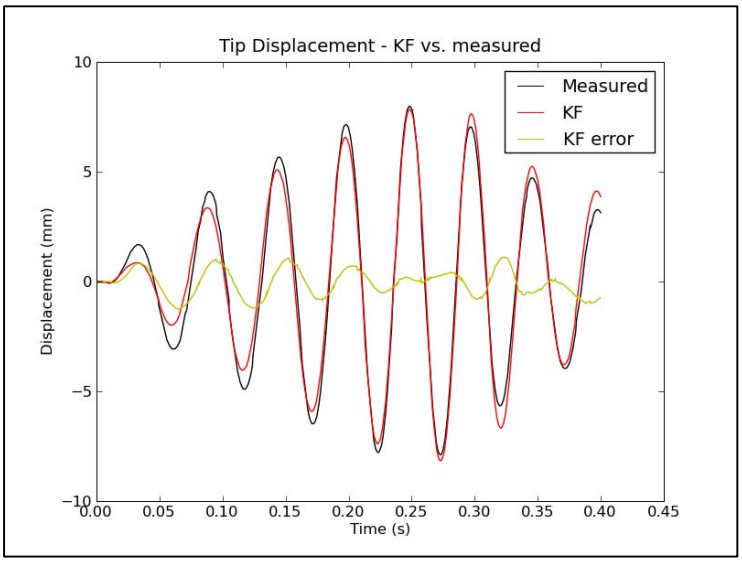

Figure 10 - Tip displacement comparison between predicted and measured values.

Given that the results of the Kalman filter simulation correlate quite well with the various references, the algorithm can be considered verified for the simple cantilever beam problem. Next, the Kalman filter must be applied to the one-meter-long wind turbine blade structure. The test set-up, shown in Figure 11, was very similar to the aluminum cantilever beam test. A laser vibrometer was placed at the end of the blade. An accelerometer and a shaker were attached 21 cm from the tip of the blade. Tests were run and acceleration data taken for a variety of sine and chirp inputs.

The next challenge was to construct the dynamic model of the blade. Geometrical properties were estimated for a five-element discretization. Material properties were unknown, so the modulus of elasticity had to be estimated. To do so, a simple finite element beam model was constructed to compare natural frequencies to the modal properties of the blade. The blade properties were found experimentally by conducting a roving impact hammer modal test. The value of the modulus of elasticity in the analytical model was then calibrated to best match the first natural frequency (which is the mode excited the most in the Kalman filter testing). A modulus of E = 17 GPa was settled on, which yielded an error of about 1% in the frequency of the first mode.

Figure 11 - Wind turbine test set-up for Kalman filter validation.

However, the first round of simulations did not give good results. Such a difficulty indicates that a more accurate model of the turbine blade is needed. Because of the irregular geometry and unknown material, the current model estimates the mass and stiffness properties of the blade rather crudely. In order to produce meaningful results, a more detailed model of the turbine blade must be developed.

This difficulty will undoubtedly arise in the real turbine blade application as well, highlighting the need for understanding the uncertainty in the various parameters used in the Kalman filter algorithm. Therefore, a verification and validation (V&V) study will be performed on the turbine blade test structure to demonstrate how parameter estimation would be accomplished in a real-world application. First, the important parameters are selected with the aid of a Phenomenon Identification and Ranking Table (PIRT). The parameters with a high “UxS” factor, which represents the combination of factors that have high uncertainty and on which the solution is sensitive, will be assessed to see how they may be improved. Performing a sensitivity analysis will be particularly important to establish how the solution error changes as parameters are changed.

Conclusions

A low-cost smart washer has been demonstrated as an effective impedance sensor for detecting damage in the hub of a CX-100 wind turbine. The repeatability of the smart washers eliminates the need for a baseline measurement when implementing multiple washers, making smart washers ideal for wind turbine application. Because of this minimal baseline requirement, a simple statistical model for estimating bolt torque was developed by extracting the damping ratio of impedance measurements. After establishing a model, an advance-warning system was developed by which the parameters were defined so that turbine blade operators would successfully be able to identify undamaged bolted connections, damaged bolted connections, and bolted connections that could potentially become damaged soon if not attended to.

Sources of error in the model were identified as coming from the torque measurements. Finding a suitable vibration isolator for the washer which would also allow a consistent bolt load to be maintained would help improve model variance and result in more accurate torque estimation. Future work would include improving the torque measurements and validating the statistical model and the warning system in an actual turbine hub.

The Kalman filter technique for measuring tip deflection has made substantial progress toward implementation on wind turbine blades. The algorithm was selected to make dynamic estimations of tip deflection using only acceleration data and a model of the structure. It is particularly well suited to the wind turbine application because it requires no knowledge of the input force or of the initial conditions and can tolerate substantial error in the input parameters. For a wind turbine, with its complex loading conditions, geometry, and material properties, these advantages are critical for obtaining a good estimate.

The algorithm was first implemented in Python code. The code was tested on the analytical 2-DOF spring-mass-damper system and the results matched the known solution. The aluminum cantilever beam was used to generate actual test data for the Kalman filter. Again, the algorithm performed well, predicting the peak deflection to within 2.0%. Finally, a model was constructed for the one-meter-long turbine blade. It was determined after data was taken that the system model requires significant refinement to better comprehend the complex geometrical and material properties. A sensitivity analysis will be performed to quantify the effect that uncertainty in various parameters has on the final solution. After the final two steps—improvement of the model and sensitivity analysis—the technique will be ready for application on full-scale, in-situ wind turbine blades. In short, dynamic tip displacement can be obtained by only measuring acceleration with proper application of a Kalman filter to an appropriate model of the system.

Acknowledgments

The authors would like to thank Dr. Charles Farrar and the Los Alamos Dynamics Summer School for the opportunity to conduct this research. The following companies generously provided various software packages to aid in modeling and data analysis: Vibrant Technologies, SIMULIA, and Enthought. The authors would also like to acknowledge, Abraham Light-Marquez (New Mexico Tech) and Alexandra Sobin (Daniel Webster College) for their assistance. Finally, the authors would like to thank by Mark Rumsey from Sandia National Laboratory for providing the test structure and guidance of this research.

References

1. Energy, U.S. Department of. "20% Wind Energy by 2030: Increasing Wind Energy's Contribution to U.S. Electricity Supply." July 2008. Wind & Hydropower Technologies Program. <http://www1.eere.energy.gov/windandhydro/pdfs/41869.pdf>.

2. Hahn, Berthold, Michael Durstewitz, Kurt Rohrig. "Reliability of Wind Turbines." Joachim Peinke, Peter Schaumann and Stephan Barth. Wind Energy. Springer Berlin Heidelberg, 2007.

3. Ciang, Chia Chen, Jung-Ryul Lee, and Hyung-Joon Bang. "Structural health monitoring for a wind turbine system: a review of damage detection methods." Measurement Science and Technology (2008).

4. Mascarenas, D.L., Park, G., Farinholt, K.M., Todd, M.D., Farrar, C.R., 2009, “A Low-Power Wireless Sensing Device for Remote Inspection of Bolted Joints,” *Journal of Aerospace Engineering, Part G of the Proceedings of the Institution of Mechanical Engineers*, Vol.233, No. 5, pp. 565-575.

5. Operation and Maintenance Costs for Wind Turbines. 12 May 2003. <http://www.windpower.org/EN/tour/econ/oandm.htm>.

6. Park, Gyuhae, Hoon Sohn, Charles R. Farrar, and Daniel J. Inman. "Overview of Piezoelectric Impedance-Based Health Monitoring and Path Forward." The Shock and Vibration Digest (2003): 451-463.

7. Welch, Greg and Gary Bishop. "An Introduction to the Kalman Filter." 24 July 2006. The Kalman Filter. <http://www.cs.unc.edu/~welch/media/pdf/kalman_intro.pdf>.